3-15-2016

Low-Energy (< 20 eV) and High-Energy (1000 eV) Electron-Induced Methanol Radiolysis of Astrochemical Interest

Kristal K. Sullivan

Mavis D. Boamah

Katie E. Shulenberger

Sitara Chapman

Karen E. Atkinson

See next page for additional authors

Version: Post-print

Recommended Citation

Kristal K. Sullivan, Mavis D. Boamah, Katie E. Shulenberger, Sitara Chapman, Karen E. Atkinson, Michael C. Boyer, Christopher R. Arumainayagam, "Low-Energy (< 20 eV) and High-Energy (1000 eV) Electron-Induced Methanol Radiolysis of Astrochemical Interest," Monthly Notices of the Royal Astronomical Society 460(1) (2016) 664-672.

Authors
Kristal K. Sullivan, Mavis D. Boamah, Katie E. Shulenberger, Sitara Chapman, Karen E. Atkinson, Michael C. Boyer, and Christopher R. Arumainayagam

Low-Energy (< 20 eV) and High-Energy (1000 eV) Electron-Induced Methanol Radiolysis of Astrochemical Interest

Kristal K. Sullivan,[a] Mavis D. Boamah,[a] Katie E. Shulenberger,[a] Sitara Chapman,[a] Karen E. Atkinson,[1] Michael C. Boyer,[a,2] Christopher R. Arumainayagam[a,3]

[a] Department of Chemistry,
Wellesley College,
Wellesley, MA 02481

Abstract

We report the first infrared study of the low-energy (< 20 eV) electron-induced reactions of condensed methanol. Our goal is to simulate processes which occur when high-energy cosmic rays interact with interstellar and cometary ices, where methanol, a precursor of several prebiotic species, is relatively abundant. The interactions of high-energy radiation, such as cosmic rays (E_{max} ~10^{20} eV), with matter produce large numbers of low-energy secondary electrons, which are known to initiate radiolysis reactions in the condensed phase. Using temperature programmed desorption (TPD) and infrared reflection absorption spectroscopy (IRAS), we have investigated low-energy (5–20 eV) and high-energy (~1000 eV) electron-induced reactions in condensed methanol (CH_3OH). IRAS has the benefit that it does not require thermal processing prior to product detection. Using IRAS, we have found evidence for the formation of ethylene glycol ($HOCH_2CH_2OH$), formaldehyde (CH_2O), dimethyl ether (CH_3OCH_3), methane (CH_4), carbon dioxide (CO_2), carbon monoxide (CO), and the hydroxyl methyl radical ($\bullet CH_2OH$) upon both low-energy and high-energy electron irradiation of condensed methanol at ~85 K. Additionally, TPD results, presented herein, are similar for methanol films irradiated with both 1000 eV and 20 eV electrons. These IRAS and TPD findings are qualitatively consistent with the hypothesis that high-energy condensed phase radiolysis is mediated by low-energy electron-induced reactions. Moreover, methoxymethanol (CH_3OCH_2OH) could serve as a tracer molecule for electron-induced reactions in the interstellar medium. The results of experiments such as ours may provide a fundamental understanding of how complex organic molecules (COM) are synthesized in cosmic ices.

Key words: astrochemistry – ISM: cosmic rays – radiation: dynamics – radiation mechanisms: non-thermal – molecular processes

[1] Science & Engineering Department, Bunker Hill Community College, Boston, MA 02129
[2] Current Address: Department of Physics, Clark University, Worcester, MA 01610
[3] Corresponding Author: Telephone: 781-283-3326; FAX: 781-283-3642; Email: carumain@wellesley.edu

1 Introduction

Methanol (CH_3OH) is of astrochemical interest because of its relatively high abundance in protostar environments (Maret et al. 2005), interstellar clouds (Friberg et al. 1988), and comets (Bockeleemorvan et al. 1991). Relative to that of water ice, observed interstellar methanol ice abundance values range from 1% to as high as 30% (Gibb et al. 2004; Grim et al. 1991; K. I. Oberg et al. 2011). Moreover, methanol is thought to be an important precursor not only to simple species such as methyl formate ($HCOOCH_3$) and dimethyl ether (CH_3OCH_3), but also to many prebiotic species such as simple sugars and amino acids (Allamandola and Hudgins 2000; Andrade et al. 2009; Hollis et al. 2000). It has been proposed that CH_3OH formation occurs through the successive hydrogenation of CO molecules in ice mantles encasing interstellar dust grains (Watanabe et al. 2003). Laboratory experiments simulating these processes have demonstrated the formation of formaldehyde (CH_2O) and methanol in amounts consistent with observed abundances in the interstellar medium (ISM) (Watanabe et al. 2003).

Remnants of older generations of stars, interstellar clouds of gas, dust, and ice become the building blocks of protostellar disks, from which new stars, planets, asteroids, comets, and other macroscopic objects form (Ehrenfreund and Charnley 2000; Herbst 2014; Mannings 2000). Observations at infrared, submillimetre, millimetre, and radio frequencies show that a large variety of organic molecules are present in these interstellar clouds (R.T. Garrod et al. 2008; Mannings 2000). In fact, star-forming regions within dark, dense molecular clouds are defined by a relative abundance of organic molecules such as methanol (R.T. Garrod et al. 2008). Organic molecular classes identified within these protostellar hot cores and hot corinos include nitriles, aldehydes, alcohols, acids, ethers, ketones, amines, and amides (Irvine 1987; Olano et al. 1988; van Dishoeck et al. 1993). Although the majority of identified species consist of only a few atoms, larger molecules such as fullerenes and polycyclic aromatic hydrocarbons (PAHs) have also been observed in several different regions of the interstellar medium (Allamandola and Hudgins 2000; García-Hernández et al. 2013; Mannings 2000).

Multiple reaction pathways for the formation of molecules in the ISM environment must be available given the extreme variations in interstellar physical conditions, such as densities ranging from 10^2 to 10^8 hydrogen atoms cm^{-3} and temperatures ranging from 10 to 10,000 K (Ehrenfreund and Charnley 2000; Mangum and Wootten 1993). Gas-phase reactions, surface reactions on bare dust grains, and UV-induced chemistry in ice mantles are thought to be the three main mechanisms for chemical synthesis in the interstellar medium (Charnley et al. 1992; Herbst 2014).

Barrier-less gas-phase reactions in the ISM are sufficiently efficient to account for the formation of simple species such as CO, N_2, O_2, C_2H_4, HCN, and simple carbon chains (Herbst 1995). However, studies have shown that gas-phase processes are much too inefficient to account for the observed abundance of species such as methyl formate ($HCOOCH_3$) in star-forming regions, suggesting that gas-phase processes play only a minor role in the formation of more complex species (Horn et al. 2004). Although surface reactions on carbonaceous or silicaceous dust grains in diffuse interstellar clouds are responsible for the synthesis of molecular hydrogen (Vidali 2013), experiments of surface hydrogenation reactions have shown the favoured mechanism to be the dissociation, rather than the synthesis, of complex molecules (Bisschop et al. 2007). Thus, surface reactions on bare dust grains may serve to slow the build-up of complex molecules. In contrast, in ice mantles surrounding dust grains found in cold, dark, dense molecular clouds, synthesis of

complex organic molecules is thought to occur via both surface and bulk reactions.

According to a recent publication, "models show that photochemistry in ices followed by desorption may explain the observed abundances" of gas-phase complex molecules detected in hot cores (K.I. Oberg et al. 2009). The interstellar UV radiation field, however, is not able to penetrate into the dark interior of dense molecular clouds (Prasad and Tarafdar 1983). Following excitation by secondary electrons produced by cosmic rays, H_2 molecules decay to the ground electronic state by emitting UV photons, leading to a cosmic ray-induced UV radiation field within the dark, dense molecular clouds (Prasad and Tarafdar 1983). These cosmic ray-induced UV photons are thought to photoprocess ice mantles surrounding dust grains within the protostar environment (Prasad and Tarafdar 1983).

In addition to UV light, high-energy radiation (e.g., cosmic rays and γ-rays) is also incident on interstellar ices. The interaction of high-energy radiation with condensed matter results in the formation of copious numbers (~ 4×10^4 electrons per MeV of energy deposited) of low-energy secondary electrons, which form distinct energetic species that are thought to promote a variety of radiation-induced chemical reactions (Kaplan and Miterev 1987). The majority of these secondary electrons have energies below 15 eV, and dissociate neutral molecules via one of three mechanisms: (1) dissociative electron attachment (DEA), (2) electron impact excitation, or (3) electron impact ionization (Arumainayagam et al. 2010). The three electron-induced molecular dissociative mechanisms are illustrated below for a generic neutral molecule AB.

$$e^- + \mathrm{AB} \rightarrow \mathrm{AB}^{-*} \rightarrow {}^{\cdot}\mathrm{A} + \mathrm{B}^- \quad (1)$$

$$e^- + \mathrm{AB} \rightarrow \mathrm{AB}^{*} + e^- \rightarrow {}^{\cdot}\mathrm{A}^{*} + {}^{\cdot}\mathrm{B} \quad (2)$$

$$e^- + \mathrm{AB} \rightarrow \mathrm{AB}^{+*} + 2e^- \rightarrow {}^{\cdot}\mathrm{A} + \mathrm{B}^{+*} + 2e^- \quad (3)$$

Dissociative electron attachment (equation 1), a resonant process occurring at low electron energies (0 to 15 eV), is characterized by the initial capture of an electron by a molecule to form a transient negative ion, which subsequently dissociates into a radical and an anion (Arumainayagam et al. 2010). Unlike electrons, photons cannot be captured into

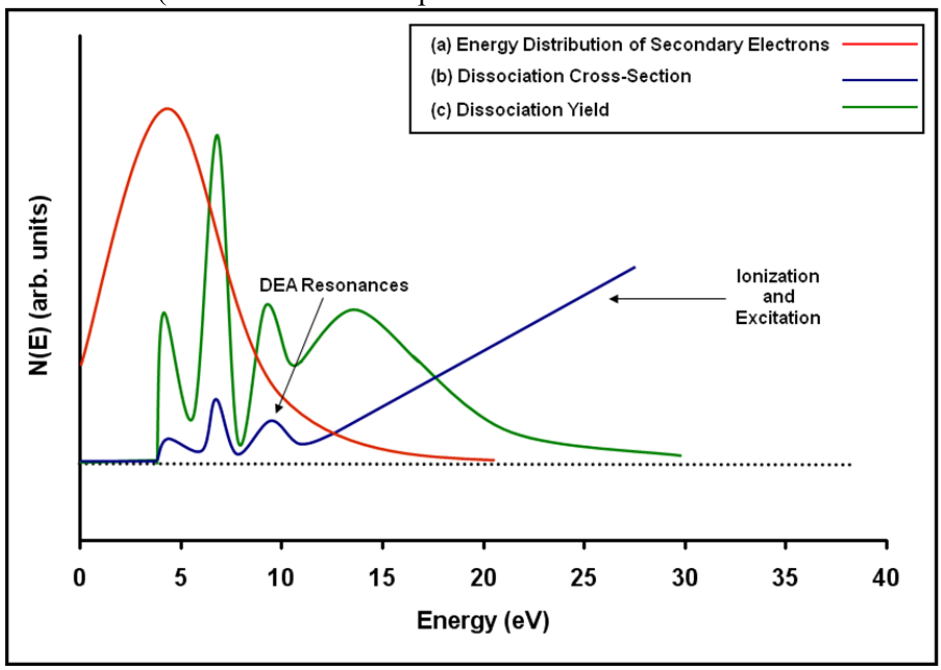

Fig. 1: Schematic of (a) energy distribution of secondary electrons generated during a primary ionizing event; (b) cross-section for electron-induced dissociation for a typical molecule; (c) dissociation yield as a function of electron energy for a typical molecule (Rajappan et al. 2010).

resonant negative ion states. In contrast, both photons and electrons can induce excitation and ionization. Electron impact electronic excitation followed by dipolar dissociation (equation 2) and electron impact ionization followed by fragmentation (equation 3) occur at electron energies typically above 3 eV and 10 eV, respectively.

The secondary electrons resulting from the interaction of high-energy radiation (e.g., cosmic rays) with matter are characterized by the majority of electrons having energies below ∼15 eV (Fig. 1(a)). For a generic molecule, the dissociation cross-section as a function of incident electron energy (Fig. 1(b)) shows resonances due to dissociative electron attachment at low (< 15 eV) electron energies, followed by a monotonic increase at higher electron energies due to available electron impact excitation and ionization dissociation pathways. Multiplying the secondary electron energy distribution by the dissociation cross-section gives the dissociation yield as a function of electron energy (Fig. 1(c)). Even though the dissociation probability increases above a threshold of ∼10 eV for a typical molecule, the yield function indicates that dissociation due to secondary electrons is far more likely at energies below ∼15 eV (Arumainayagam et al. 2010). According to a recent publication, "it is appropriate to suggest that low-energy electrons are the most important species in radiation chemistry" (Pimblott and LaVerne 2007).

Processing of interstellar, cometary, and planetary ices likely involves high-energy radiation-induced low-energy electrons. While the mean free paths of low-energy (18–68 eV) electrons in condensed water and methanol are ~ 13 Å and ~ 10 Å, respectively (Kurtz et al. 1986), the penetration depth of light ions can be as high as 10^6 μm in interstellar ices, which are typically less than 1 μm thick (de Barros et al. 2014). Therefore, we propose that cosmic-ray-induced low-energy electron processing of interstellar ices may occur via three mechanisms (Cuppen 2014): (1) the interaction of cosmic rays with gaseous molecular hydrogen produces low-energy electrons that can interact with the surface (top few molecular layers) of cosmic ices, (2) the interaction of cosmic rays with molecules within ices generates a cascade of low-energy electrons which can interact with the surface and the bulk of the ice mantles, (3) the interaction of the cosmic rays with the dust grain beneath the ice mantle engenders low-energy electrons that can interact with the bottom ice layers in contact with the dust grain.

Based on post-irradiation temperature programmed desorption experiments, we have recently shown that low-energy (< 20 eV) electron processing of methanol ices essentially produces the same products as UV photolysis of condensed methanol (Boamah et al. 2014). In the work presented herein, we have extended our previously published work to include the use of post-irradiation IR for product identification. While both techniques allow us to identify the radiolysis products of methanol, in contrast to temperature programmed desorption, IRAS has an advantage in that it does not require thermal processing prior to product detection. In addition, we have extended our studies of low-energy (< 20 eV) electrons to high-energy (1000 eV) electrons. In the post-irradiation temperature programmed desorption and infrared spectroscopy results presented herein, we demonstrate that the same radiolysis products result from irradiation of condensed methanol with low-energy (< 20 eV) and high-energy (~ 1000 eV) electrons. These qualitative findings indicate that high-energy radiation-induced changes may be attributable to low-energy secondary electron interactions with condensed matter. Hence, our results suggest that cosmic-ray-induced low-energy electrons very likely play an important role in the synthesis of complex molecules in the interstellar medium.

2 Experimental Section

Experiments were performed in a custom-designed stainless steel ultrahigh vacuum (UHV) chamber with a base pressure of 5×10^{-10} Torr, previously described in detail (Harris et al. 1995). A Mo(110) single crystal substrate was mounted on a precision sample manipulator capable of *x*-, *y*-, and *z*- translations. Polar rotation of the crystal mount was provided by a differentially-pumped rotary feedthrough. The crystal substrate could be cooled to ~85 K with liquid nitrogen and heated to 800 K radiatively or to 2200 K by electron bombardment. Temperature measurements were made using a tungsten-rhenium, W-5% Re vs. W-26% Re thermocouple spot welded to the edge of the crystal. The crystal was routinely cleaned by heating to 2200 K, exceeding the desorption temperature of oxygen.

All samples [CH_3OH (Aldrich, 99.9+ %), $^{13}CH_3OH$ (Aldrich, 99%), CH_3CH_2OH (Pharmco, anhydrous absolute), $HCOOCH_3$ (Aldrich, anhydrous 99%), CH_3OCH_3 (Aldrich, 99%), $HOCH_2CH_2OH$, (Aldrich, anhydrous 99.8%) $HCOCH_2OH$ (Aldrich, crystalline dimer), CH_3COOH (EMD, glacial)] were stored in cleaned (baked) Schlenk tubes and degassed by three freeze-pump-thaw cycles before use. The two exceptions were: (1) $HCOCH_2OH$, a solid dimer sample which was gently heated to produce monomer fragments before introduction to the chamber, and (2) CH_3OCH_3, which was packaged in a pressurized canister and introduced directly into the UHV chamber.

Dosers with precision leak valves allowed for controlled deposition of methanol onto the Mo(110) crystal surface. Temperature programmed desorption experiments in the absence of electron irradiation were used to determine the coverage of CH_3OH. One monolayer (1 ML) is defined as the coverage achieved by the maximum exposure of the adsorbate that does not yield a multilayer peak. Film thickness (20–100 ML) was sufficient to rule out any contribution from Mo surface interactions. To minimize charging of films during irradiation with low-energy electrons, we used 20 ML films for post-irradiation temperature programmed desorption experiments. For better signal to noise ratio, we used 100 ML films for post-irradiation IRAS experiments. Multilayers of methanol at 85 K form an amorphous solid (glass), because crystallization of methanol occurs only above 128 K (Dempster and Zerbi 1971).

An FRA-2X1-2 electron gun (Kimball Physics Inc.) was used to irradiate condensed methanol films on the crystal substrate. The transmitted current was set at 2.0 μA (electron dose of 2.4×10^3 μC) on the clean crystal for most experiments. Incident electron energy was varied between 5 and 1000 eV. Our choice of 5 eV for the minimum incident electron energy was dictated by the fact that at electron energies below ~ 10 eV, electron impact ionization is not a viable mechanism for product formation.

Post-irradiation infrared reflection absorption spectroscopy measurements were performed using a recently installed TENSOR™ 27 FTIR spectrometer (Bruker Optics) equipped with a liquid nitrogen-cooled mercury cadmium telluride (MCT) detector. A background spectrum (1000 scans at 8 cm^{-1} resolution) of the clean crystal was subtracted from all sample IRAS spectra. Unless otherwise noted, all sample spectra were collected at 8 cm^{-1} resolution with coaddition of 250 scans for each spectrum.

After irradiation of methanol films with electrons, temperature programmed desorption measurements were also performed using a Hiden IDP Series 500 quadrupole mass spectrometer. Five or fewer mass-to-charge ratios were monitored during typical temperature programmed desorption experiments in order to optimize the signal-to-noise ratio while allowing for identification of radiolysis products. Temperature programmed desorption experiments

conducted in the absence of electron irradiation served as control experiments.

3 Results and Discussion

Multiple methods based on infrared reflection absorption spectroscopy were utilized to identify low- and high-energy electron-induced nascent radiolysis products formed at 85 K within methanol thin films. First, IR peak positions were compared to previously published values for the radiolysis/photolysis products of condensed methanol. Second, these peak assignments were further verified by annealing experiments during which the irradiated CH_3OH thin film was heated to various temperatures before IR analysis at 85 K. The temperatures corresponding to the loss of IR peaks were compared with previously recorded radiolysis product desorption temperatures (Boamah et al. 2014; Harris et al. 1995). Third, mixtures of CH_3OH with approximately 10–30% of the potential radiolysis product were dosed onto the crystal at 85 K. IR spectra of these unirradiated, mixed thin films were used as additional evidence for peak assignments in electron-irradiated condensed methanol. Fourth, IR spectra of irradiated $^{13}CH_3OH$ were used to further verify radiolysis product identifications for species such as CO and CO_2, which are significant contaminants in ultrahigh vacuum chambers.

As described in detail elsewhere (Boamah et al. 2014), the identifications of electron-induced methanol radiolysis species via post-irradiation temperature programmed desorption were based on (1) comparison to known mass spectra, (2) temperature programmed desorption data for methanol films containing the suspected radiolysis product, (3) results of analogous experiments with methanol isotopologues ($^{13}CH_3OH$ and CD_3OD), and (4) trends in boiling points and desorption temperatures. Despite the use of these methods, several of our identifications of electron-induced methanol radiolysis products are not unambiguous because of (1) the multitude of methanol radiolysis products, (2) small reaction yields which were dependent on film thickness, irradiation time, and incident electron energy, (3) closeness in desorption temperatures of some radiolysis products, and (4) the inability to monitor mass spectral fragments (e.g., $m/z = 31$) that were common to both methanol and some radiolysis products. Results of temperature programmed desorption experiments conducted following high-energy (1000 eV) and low-energy (20 eV) electron irradiation of methanol thin films are shown in Fig.2 and Fig.3, respectively. To improve clarity, not all mass spectral fragments monitored are shown in these two figures. As a result, positions of some vertical lines used to identify peaks are not obvious in Figure 3.

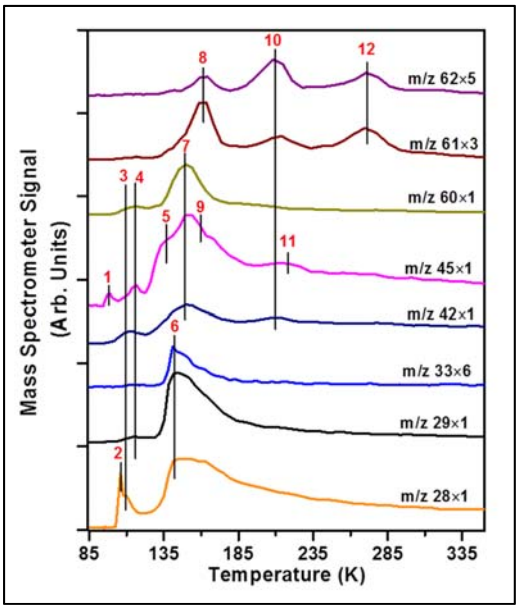

Fig. 2: Post irradiation temperature programmed desorption data for 20 monolayers of $^{12}CH_3OH$ irradiated with 1000 eV electrons for 5 seconds at a transmitted current of 2 μA (flux ≈ 2×10^{13} electrons/cm^2/s and fluence ≈ 1×10^{14} electrons/cm^2) show several desorption features: (1) dimethyl ether (CH_3OCH_3), (2) carbon monoxide (CO), (3) methyl formate ($HCOOCH_3$), (4) glycolaldehyde ($HOCH_2CHO$), (5) unknown, (6) methanol, (7) acetic acid (CH_3COOH), (8) methoxymethanol (CH_3OCH_2OH), (9) ethanol (CH_3CH_2OH), (10) ethylene glycol ($(CH_2OH)_2$), (11) glycolic acid ($HOCH_2CO_2H$), (12) 1,2,3-propanetriol ($HOCH_2CHOHCH_2OH$, glycerol). Plots vertically offset for clarity.

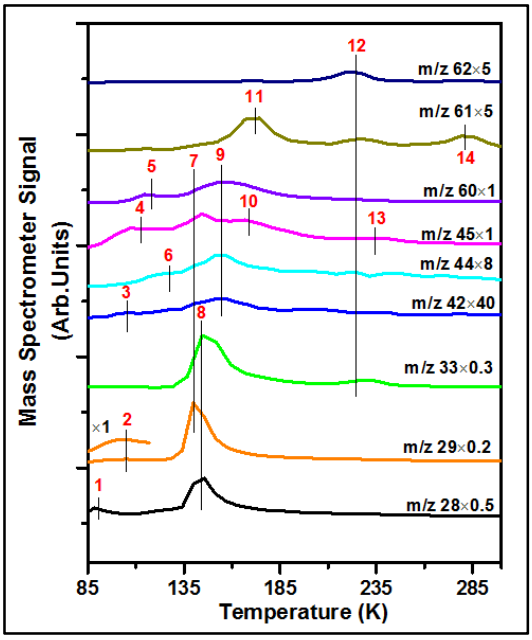

Fig. 3: Post irradiation temperature programmed desorption data for 20 monolayers of $^{12}CH_3OH$ irradiated with 20 eV electrons for 20 minutes at a transmitted current of 2 μA (flux ≈ 2×10^{13} electrons/cm^2/s and fluence ≈ 3×10^{16} electrons/cm^2) show several desorption features: (1) CO (background), (2) formaldehyde (H_2CO), (3) unknown, (4) dimethyl ether (CH_3OCH_3), (5) methyl formate ($HCOOCH_3$), (6) acetaldehyde (CH_3CHO), (7) glycolaldehyde ($HOCH_2CHO$), (8) methanol (CH_3OH), (9) acetic acid (CH_3COOH), (10) ethanol (CH_3CH_2OH), (11) methoxymethanol (CH_3OCH_2OH), (12) ethylene glycol ($(CH_2OH)_2$), (13) glycolic acid ($HOCH_2CO_2H$), (14) 1, 2, 3-propanetriol ($HOCH_2CHOHCH_2OH$). Plots vertically offset for clarity (Boamah et al. 2014).

3.1 Ethylene Glycol ($HOCH_2CH_2OH$) Formation

Based on the results of post-irradiation temperature programmed desorption, ethylene glycol was identified as a radiolysis product following irradiation of condensed methanol with high-energy (1000 eV) electrons (Fig. 2). We have previously demonstrated that irradiation of methanol ices by electrons with energies as low as 5 eV results in the formation of ethylene glycol (Boamah et al. 2014).

Even in the absence of the thermal processing characteristic of temperature programmed desorption, post-irradiation IR spectra demonstrate the formation of ethylene glycol ($HOCH_2CH_2OH$) at 85 K upon low-energy (20 eV) and high-energy (900 eV) electron irradiation of condensed methanol (Fig. 4). Ethylene glycol formation at 85 K was verified by the presence of a prominent IR peak at ~1092 cm^{-1}, as well as weaker peaks at ~890 and ~865 cm^{-1}, observed following electron irradiation of condensed methanol. Ethylene glycol production was observed via IR spectroscopy when methanol films were irradiated with electrons with energies as low as 7 eV (electron dose of 2.4×10^3 μC), suggesting that electron impact ionization cannot be the sole mechanism for ethylene glycol formation. During annealing experiments, IR peaks associated with ethylene glycol disappeared between 200 and 250 K, consistent with the ~210 K ethylene glycol desorption temperature found during temperature programmed desorption following low-energy electron irradiation of condensed methanol. Furthermore, IR spectra of thin films formed from a mixture of ~10% (v/v) ethylene glycol in CH_3OH dosed onto the Mo(110) crystal at 85 K evinced prominent peaks that were consistent with features attributed to ethylene glycol in the irradiated CH_3OH thin film. Our IR identification of ethylene glycol formation following low- and high-energy electron irradiation of condensed methanol is consistent with previous IR studies involving high-energy electrons (Bennett et al. 2007), UV (Gerakines et al. 1996; K.I. Oberg et al. 2009), X-ray (Chen et al. 2013), and proton (Hudson and Moore 2000) irradiation of methanol ices.

Methanol radiolysis leading to ethylene glycol formation has been previously attributed to the dimerization of two hydroxymethyl (•CH_2OH) radicals (Getoff et al. 1993). The absence of ethylene glycol in high-energy electron-irradiated methanol ice at 30 K (Jheeta et al. 2013) is consistent with heavy radicals such as hydroxymethyl radicals requiring higher

temperatures for facile diffusion. Given that copious numbers of low-energy electrons are produced by the interactions of high-energy radiation, electron impact electronic excitation is likely the dominant mechanism for the formation of hydroxymethyl radicals during the high-energy radiolysis of methanol, as we have described in detail elsewhere (Boyer et al. 2014).

3.2 Formaldehyde (H_2CO) Formation

Formaldehyde (H_2CO) formation at 85 K following electron irradiation of condensed methanol was confirmed by IR peaks at 1724 and 1250 cm^{-1} (Fig. 4). Formation of formaldehyde was seen after irradiation with electrons with energies as low as 9 eV (electron dose of 2.4 $\times 10^3$ μC). Results of annealing experiments showed the disappearance of formaldehyde IR peaks between 120 and 135 K, slightly above the desorption temperature of ~115 K reported in our previous post-irradiation temperature programmed desorption study of condensed methanol (Boamah et al. 2014). The prominent IR peak at 1724 cm^{-1} has been observed following radiolysis/photolysis of condensed methanol (Allamandola et al. 1988; Baratta et al. 2002; Chen et al. 2013; de Barros et al. 2011; Gerakines et al. 1996; Hudson and Moore 2000; Jheeta et al. 2013; K.I. Oberg et al. 2009; Palumbo et al. 1999).

Formaldehyde is thought to be produced through the combination of •H and •HCO radicals and/or disproportionation of the hydroxymethyl radicals within the irradiated CH_3OH thin film (Getoff et al. 1993). Facile •H radical diffusion possible at ~10 K (Watanabe et al. 2003) probably accounts for the detection of formaldehyde at temperatures as low as 11 K following irradiation of condensed methanol with high-energy (5000 eV) electrons (Bennett et al. 2007).

3.3 Dimethyl Ether (CH_3OCH_3) Formation

Results of temperature programmed desorption experiments conducted following high-energy (1000 eV) electron irradiation of condensed CH_3OH demonstrated desorption features which we attribute to dimethyl ether (Fig.

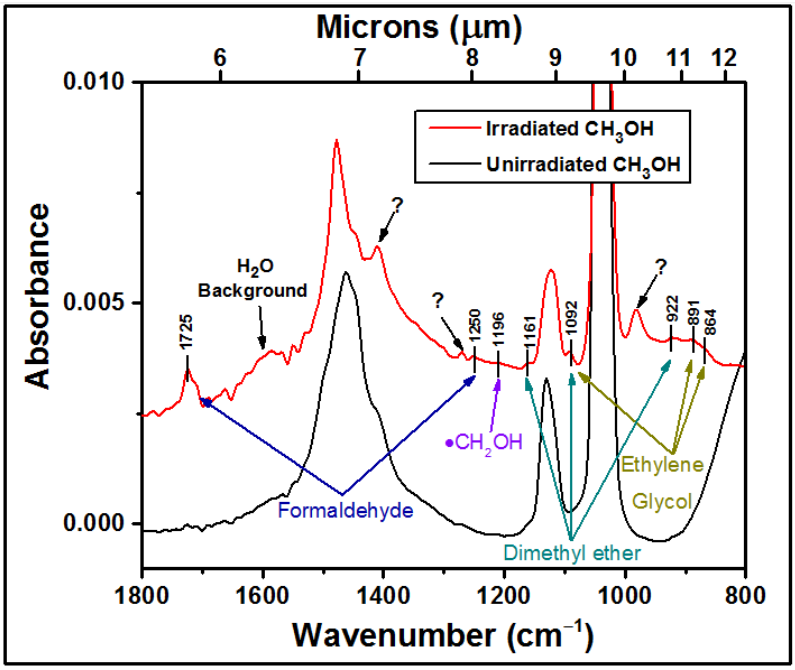

Fig. 4: IRAS spectra of 100 ML of unirradiated (black curve) and irradiated (14 eV electrons for 20 minutes at a transmitted current of 2 μA) (red curve) condensed CH_3OH.

2). We have previously demonstrated that irradiation of methanol ices by electrons with electron energies as low as 7 eV results in the formation of dimethyl ether (Boamah et al. 2014).

The electron-induced production of dimethyl ether (CH_3OCH_3) at 85 K from condensed methanol was confirmed by the prominent IR peak at 1092 cm^{-1} as well as weaker peaks at 1161 and 922 cm^{-1} (Fig. 4). Formation of this product was seen after irradiation with electrons with energies as low as 7 eV (electron dose of 2.4×10^3 μC), suggesting that electron impact ionization cannot be the sole mechanism for dimethyl ether formation. During annealing experiments, IR peaks at 1161 and 922 cm^{-1}, associated exclusively with CH_3OCH_3, began to disappear at ~100 K, consistent with results of post-irradiation temperature programmed desorption.

In previous IRAS studies of irradiated CH_3OH, the peaks at 1161 and 922 cm^{-1} were attributed to either dimethyl ether (K.I. Oberg et al. 2009) or another methanol radiolysis product, methyl formate ($HCOOCH_3$) (Bennett et al. 2007; Gerakines et al. 1995; Palumbo et al. 1999). In order to resolve this discrepancy, IR spectra of condensed films of a mixture of ~20% (v/v) dimethyl ether in CH_3OH were compared to those of a mixture of ~30% (v/v) methyl formate in CH_3OH. IR peaks of the dimethyl ether/CH_3OH thin film better matched those of the electron

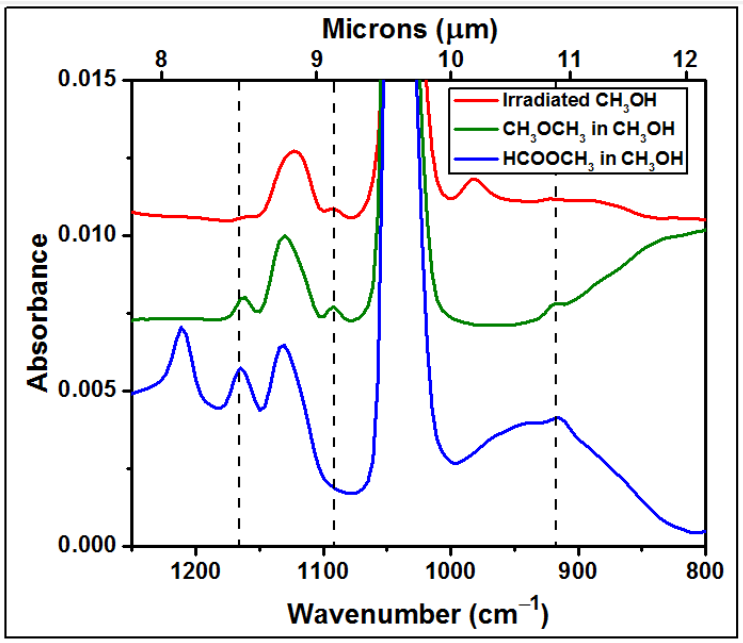

Fig. 5: IRAS scan of (1) 100 ML of CH_3OH after irradiation with 14 eV electrons for 20 minutes at a transmitted current of 2 μA (red curve), (2) CH_3OH / CH_3OCH_3 (dimethyl ether) mixture (green curve), (3), CH_3OH / $HCOOCH_3$ (methyl formate) mixture (blue curve).

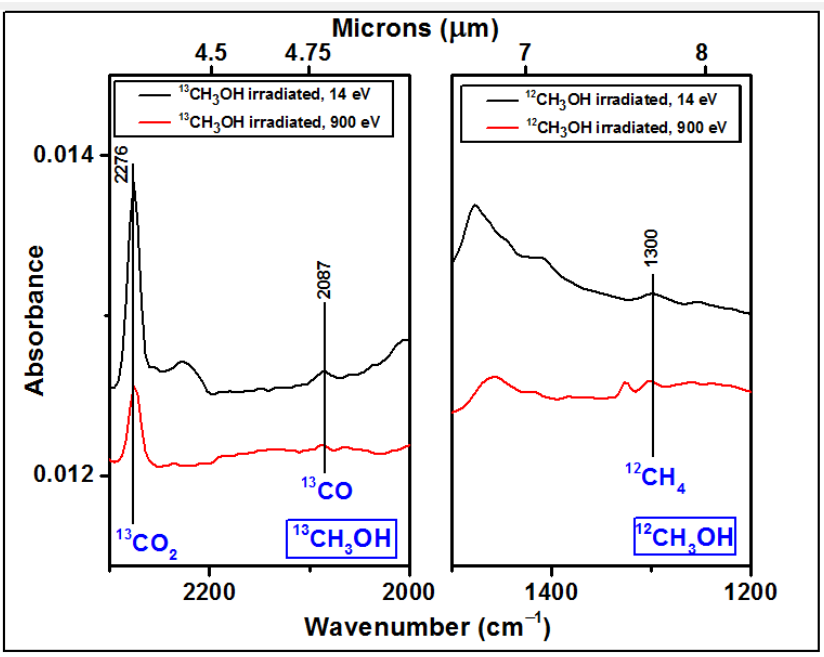

Fig. 6: IRAS scan of 100 ML of $^{13}CH_3OH$ (left panel) and $^{12}CH_3OH$ (right panel) irradiated with 14 eV electrons for 120 minutes at a transmitted current of 2 μA (black curve) and with 900 eV electrons for 2 minutes at a transmitted current of 0.5 μA (red curve).

irradiated CH_3OH ice (Fig. 5). Although IR features of the methyl formate also align well with features in the irradiated CH_3OH sample, particularly the band at 1161 cm^{-1}, the absence of the even more prominent methyl formate peak at 1207 cm^{-1} in the irradiated CH_3OH sample supports our IR peak assignments (Chen et al. 2013).

Dimethyl ether formation likely occurs via radical-radical reactions involving CH_3O• and •CH_3 radicals (Bennett et al. 2007).

3.4 Hydroxymethyl radical (•CH_2OH) Formation

Consistent with the results of multiple previous IRAS studies of irradiated methanol ices (Bennett et al. 2007; de Barros et al. 2011; Gerakines et al. 1996; K.I. Oberg et al. 2009), the hydroxymethyl radical (•CH_2OH) was identified at 85 K by a single weak peak at 1195 cm^{-1} following high-energy and low-energy electron irradiation of condensed methanol. Tentative evidence for the production of hydroxymethyl radical was only seen after irradiation with 14 eV electrons (electron dose of 2.4 × 10^3 μC) (Fig. 4),[4] although formation of $HOCH_2CH_2OH$ was detected at energies as low as 7 eV. The observed difference in threshold incident electron energy may be due to a higher minimum IR detectability of hydroxymethyl radical compared to that of ethylene glycol. Hydroxymethyl radical has been identified in several methanol radiolysis studies involving electron spin resonance (ESR) spectroscopy studies following spin trapping (Spinks and Woods 1990).

3.5 CO_2 Formation

Using IRAS, carbon dioxide (CO_2) was detected following both high-energy

[4] More conclusive IR evidence for the production of hydroxymethyl radicals was seen following irradiation of methanol ices with higher energy (> 17 eV) electrons.

and low-energy electron irradiation of methanol ices. IR evidence for CO_2 production when condensed methanol was irradiated with low-energy (14 eV) electrons was detected only following a high total electron dose of 1.4×10^4 μC. Background signals for CO_2 present in our experimental setup necessitated the use of $^{13}CH_3OH$ in order to detect IR peaks uniquely attributable to carbon dioxide produced from the radiolysis of methanol. A prominent IR peak at 2276 cm^{-1} was assigned to $^{13}CO_2$ (Fig. 6), in good agreement with literature values (Table 1) (Gerakines et al. 1996). Carbon dioxide is thought to be produced by the reaction of CO and the hydroxyl radical (•OH) formed during the radiolysis of methanol (R. T. Garrod and Herbst 2006).

3.6 CO Formation

Irradiation of methanol ices by both high- and low-energy electrons resulted in the formation of carbon monoxide (CO), as shown by IRAS results. Similar to CO_2, an IR peak attributable to carbon monoxide was detected at 85 K only after irradiation of condensed methanol with a high total electron dose (1.4×10^4 μC) of low-energy (14 eV) electrons. A much smaller dose of 60 μC with higher energy (900 eV) electrons incident on condensed methanol was sufficient to generate CO. A single IR peak in both irradiated CH_3OH (at 2134 cm^{-1}) (data not shown) and $^{13}CH_3OH$ (at 2087 cm^{-1}) (Fig. 6) thin films was attributed to carbon monoxide, in good agreement with previously published values (Table 1) (Allamandola et al. 1988; Baratta et al. 2002; de Barros et al. 2011; Gerakines et al. 1996; Hudson and Moore 2000; K.I. Oberg et al. 2009; Palumbo et al. 1999). Dissociation of the formyl radical (•HCO) is thought to yield CO (K.I. Oberg et al. 2009).

3.7 CH_4 Formation

Using IRAS, methane (CH_4) was detected following both high-energy and low-energy electron irradiation of methanol ices. A high total electron dose (1.4×10^4 μC) was also necessary to detect formation of methane in CH_3OH thin films irradiated with low energy (14 eV) electrons at 85 K. We attribute the detection of methane at such a high temperature to methane trapping within methanol ices. A single IR peak at 1303 cm^{-1} was attributed to CH_4 (Fig. 6), in good agreement with previously published values (Table 1) (Allamandola et al. 1988; Baratta et al. 2002; de Barros et al. 2011; Gerakines et al. 1996; Hudson and Moore 2000; K.I. Oberg et al. 2009; Palumbo et al. 1999). Methane formation is ascribed to the combination of $•CH_3$ and •H radicals (K.I. Oberg et al. 2009).

3.8 Reconciling Post-Irradiation IR and Temperature Programmed Desorption Data

As described in detail in our previous publication (Boamah et al. 2014), results of temperature programmed desorption experiments conducted following 20 eV electron irradiation of condensed methanol indicate the formation of several additional products: acetaldehyde (CH_3CHO), methyl formate ($HCOOCH_3$), glycolaldehyde ($HOCH_2CHO$), acetic acid (CH_3COOH), methoxymethanol (CH_3OCH_2OH), ethanol (CH_3CH_2OH), glycolic acid ($HOCH_2CO_2H$), and 1,2,3-propanetriol ($HOCH_2CHOHCH_2OH$, glycerol). Following 1000 eV electron irradiation of methanol ices, we have identified using temperature programmed desorption experiments (Fig. 2) all the above mentioned products, except acetaldehyde. We attribute this discrepancy to the challenges associated with using temperature programmed desorption, and conclude that post-irradiation temperature programmed desorption results indicate

Table 1:

		This Work	Jheeta et al. 2013	Bennet et al. 2007	Allamandola et al. 1988	Oberg et al. 2009	Gerakines et al. 1996	Chen et al. 2013	Hudson and Moore 2000	Palumbo et al. 1999	Baratta et al. 2002	de Barros et al. 2011
		Electrons 14 eV	Electrons 1 keV	Electrons 5 keV	UV	UV	UV	X-rays ~400 eV	Protons 0.8 MeV	He^+ ions 3 keV	He^+ ions 3 keV	Ions 16–774 MeV
	Temperature	85 K	30 K	11 K			10–230 K	14–210 K	16 K	10–200 K	10–20 K	15 K
ν_4	**CH_2OH**	1195	1345(?)	1192		1195	1197	1193				1193
ν_4	**H_2CO**	1724	1724	1726	1720	1727	1719	1726	1712	1720	1720	1726
ν_3	**H_2CO**			1496	1500	1498	1497	1498	1499			1497
ν_2	**H_2CO**	1250		1245		1245	1244	1249	1248			1244
ν_1	**HCO**			1849, 1841	1850	1843	1850, 1863	1842	1848			
ν_1	**CO**	2134	2136	2134	2137	2135	2138	2134	2135	2136	2136	2136
ν_1	**CO (^{13}C)**	2087					2092					2092
ν_3	**CO_2**	2341	2341	2345	2343	2340	2342	2340	2341	2344	2344	2342
ν_3	**CO_2 (^{13}C)**	2276					2278					
ν_2	**CO_2**				657		655		654	660		
ν_4	**CH_4**	1303	1304	1303	1304	1301	1304	1304	1303	1305	1308	
ν_3	**CH_4**				3012		3011					3009
ν_{14}	**CH_3OCHO**			1718			1718	1726				
ν_{12}	**CH_3OCHO**					1214						
ν_5	**CH_3OCHO**			916		911	910					
ν_8	**CH_3OCHO**			1160			1160	1161				1160
ν_{10}	**CH_3OCH_3**	1161				1161		1161				
ν_6	**CH_3OCH_3**	914				921						
ν_9	**$HOCH_2CH_2OH$**	1092		1090		1090	1088	1090	1088			
ν_7	**$HOCH_2CH_2OH$**	891		889		890		875–932	885			
ν_6	**$HOCH_2CH_2OH$**	864		856		866			861			
ν_5	**$HOCH_2CH_2OH$**			525					524			
ν_{14}	**$HCOCH_2OH$**			1747				1746				
ν_{12}	**CH_3CH_2OH**					1382						
ν_4	**CH_3CH_2OH**					885						
ν_2	**C_2H_6**					1372						
ν_{12}	**C_2H_6**					822						
ν_7	**CH_3CHO**					1350						
ν_{18}	**CH_3COCH_3**									1720		
ν_{17}	**CH_3COCH_3**									1444		
ν_{11}	**CH_3COCH_3**									1232		
ν_{10}	**CH_3COCH_3**									1090		
ν_1	**H_2?**						4140					
ν_2	**HCOO-?**					1382			1384			
ν_5	**HCOO-?**								1589			
ν_2	**H_2O**									1655	1655	

Comparison of several studies which investigated the radiolysis/photolysis of CH_3OH thin films using IRAS. Expansion of a previously published table (Bennet et al. 2007).

the same products are formed following low-energy (20 eV) and high-energy (1000 eV) electron irradiation of condensed methanol.

While seven methanol radiolysis products were identified with IR, as described in detail in sections 3.1 to 3.7, clear IR signatures were not found for the eight products mentioned in the current section. This discrepancy between post-irradiation IR and temperature programmed desorption data is not surprising given that (1) an observed infrared feature is generally associated with normal modes of two or more atoms rather than a specific molecule, (2) IRAS signals are typically small even for surface coverages in the multilayer regime, (3) irradiated methanol contains 15 or more radiolysis products which engender a multitude of often overlapping IR peaks, (4) methoxymethanol is a labile species for which there is no IR spectrum in databases.

Despite the absence of IRAS evidence for acetaldehyde (CH_3CHO), methyl formate ($HCOOCH_3$), glycolaldehyde ($HOCH_2CHO$), methoxymethanol (CH_3OCH_2OH), and ethanol (CH_3CH_2OH) at 85 K, we suggest that thermal processing above 85 K of the irradiated methanol film is not necessary for the formation of these five products. Our reasoning is based on the assumption that barrier-less radical-radical reactions are thought to yield the photolysis/radiolysis products of methanol. Therefore, the diffusion barriers of the radicals determine the temperature dependence of product formation. Our results indicate that these five radiolysis products must form at 85 K or below given that the methoxy (CH_3O•), formyl (•HCO), and methyl (•CH_3) radicals have diffusion barriers (R.T. Garrod et al. 2008) significantly lower than that of the hydroxymethyl radical (•CH_2OH), whose dimerization yields ethylene glycol at 85 K or below, as verified by IR data presented herein.

3.9 Implications for Interstellar Chemistry

The results presented herein suggest that low-energy secondary electrons can induce chemical processes within interstellar ice films. Within protostellar environments, cosmic-ray induced low-energy secondary electrons may interact with ice films rich in CH_3OH to form radical species whose subsequent reactions may lead to the production of some of the diverse observed interstellar molecules, including prebiotic species. Because all previous studies (Allamandola et al. 1988; Gerakines et al. 1996; K.I. Oberg et al. 2009) have failed[5] to identify methoxymethanol (CH_3OCH_2OH) as a photolysis product of condensed methanol, this electron-induced product of condensed methanol (Boamah et al. 2014; Boyer et al. 2014; Harris et al. 1995; Maity et al. 2015) could serve as a tracer molecule for electron-induced reactions in the interstellar medium.

Although current astrochemical simulations model the irradiation chemistry of ice-covered interstellar dust grains by ionizing radiations such as cosmic-rays (e.g., Abdulgalil et al. 2013), no simulations have taken into account the role of low-energy secondary electrons. The kinetic (stochastic) Monte Carlo method (e.g., Chang 2005) must be modified to model the attenuation of low-energy electrons in ice, predicting both the spatial location and the nature of the energy transfer events.

4 Conclusions

We have investigated the effects of high-energy and low-energy electron

[5] It is possible that these authors did not specifically look for methoxymethanol in their UV photolysis studies. A clear non-detection of this species from the UV photolysis of condensed methanol is necessary to unambiguously identify CH_3OCH_2OH as a radiolysis tracer.

irradiation of nanoscale thin films of CH_3OH at 85 K under ultrahigh vacuum conditions. Infrared spectroscopy results indicate that ethylene glycol, formaldehyde, dimethyl ether, carbon dioxide, carbon monoxide, methane, and the hydroxymethyl radical are nascent low- and high-energy electron-induced radiolysis products of condensed methanol at 85 K. Post-irradiation temperature programmed desorption results presented herein also demonstrate that the same radiolysis products result from irradiation of condensed methanol with low-energy (< 20 eV) and high-energy (1000 eV) electrons, suggesting that high-energy radiation-induced changes are attributable to low-energy secondary electron interactions with condensed matter. We speculate that qualitatively similar results will result for analogs of cosmic methanol ices containing both CO and water. Therefore, the results presented herein may have implications for the synthesis of complex organic molecules (COM) in extra-terrestrial ices.

Acknowledgements

This work was supported by grants from the National Science Foundation (NSF grant number CHE-1012674 and CHE-1005032) and Wellesley College (Faculty awards and Brachman Hoffman small grants). Kristal K. Sullivan gratefully acknowledges funding from "Sally Etherton Cummins '58 Summer Science Research Fellowship Fund." We thank an anonymous referee for numerous constructive comments on the paper. Chris Arumainayagam dedicates this contribution to his late great grandfather, Professor Allen Abraham, who was in 1911 one of the first astronomers from Asia to be elected as a Fellow of the Royal Astronomical Society (FRAS) for his seminal contributions to calculating the trajectory of Haley's comet in 1910.

References

Allamandola, L.J., Hudgins, D.M., 2000, Solid state astrochemistry, From interstellar polycyclic aromatic hydrocarbons and ice to astrobiology.

Allamandola, L.J., Sandford, S.A., Valero, G.J., 1988, Icarus, 76, 225-52.

Andrade, D.P.P., Boechat-Roberty, H.M., Martinez, R., Homem, M.G.P., da Silveira, E.F., Rocco, M.L.M., 2009, Surf. Sci., 603, 1190-96.

Arumainayagam, C.R., Lee, H.D., Nelson, R.B., Haines, D.R., Gunawardane, R., 2010, Surf. Sci. Rep, 65, 1–44.

Baratta, G.A., Leto, G., Palumbo, M.E., 2002, A & A, 384, 343-49.

Bennett, C.J., Chen, S.-H., Sun, B.-J., Chang, A.H.H., Kaiser, R.I., 2007, Astrophys. J., 660, 1588-608.

Bisschop, S.E., Fuchs, G.W., van Dishoeck, E.F., Linnartz, H., 2007, A&A, 474, 1061.

Boamah, M.D., et al., 2014, Farad. Discuss., 168, 249-66.

Bockeleemorvan, D., Colom, P., Crovisier, J., Despois, D., Paubert, G., 1991, Nature, 350, 318-20.

Boyer, M.C., Boamah, M.D., Sullivan, K.K., Arumainayagam, C.R., Bazin, M., Bass, A.D., Sanche, L., 2014, J. Phys. Chem. C, 118, 22592-600.

Charnley, S.B., Tielens, A.G.G.M., Millar, T.J., 1992, Astrophys. J., 399, L71-L74.

Chen, Y.J., Ciaravella, A., Caro, G.M.M., Cecchi-Pestellini, C., Jiménez-Escobar, A., Juang, K.J., Yih, T.S., 2013, Astrophys. J., 778, 162.

Cuppen, H.M., 2014, Farad. Discuss., 168, 571-615.

de Barros, A.L.F., Domaracka, A., Andrade, D.P.P., Boduch, P., Rothard, H., da Silveira, E.F., 2011, MNRAS, 418, 1363-74.

de Barros, A.L.F., da Silveira, E.F., Pilling, S., Domaracka, A., Rothard, H.,

Boduch, P., 2014, MNRAS, 438, 2026-35.
Dempster, A.B., Zerbi, G., 1971, J. Chem. Phys., 54,
Ehrenfreund, P., Charnley, S.B., 2000, Annu. Rev. Astron. Astrophys., 38, 427-83.
Friberg, P., Hjalmarson, A., Madden, S.C., Irvine, W.M., 1988, A & A, 195, 281-89.
García-Hernández, D.A., Cataldo, F., Manchado, A., 2013, MNRAS, 434, 415-22.
Garrod, R.T., Herbst, E., 2006, A & A, 457, 927-36.
Garrod, R.T., Widicus, S.L., Herbst, E., 2008, Astrophys. J., 682, 283.
Gerakines, P.A., Schutte, W.A., Ehrenfreund, P., 1996, A&A, 312, 289-305.
Gerakines, P.A., Schutte, W.A., Greenberg, J.M., van Dishoeck, E.F., 1995, A&A, 296, 810.
Getoff, N., Ritter, A., Schworer, F., Bayer, P., 1993, Radiat. Phys. Chem., 41, 797-801.
Gibb, E.L., Whittet, D.C.B., Boogert, A.C.A., Tielens, A.G.G.M., 2004, ApJS, 151, 35-73.
Grim, R.J.A., Baas, F., Geballe, T.R., Greenberg, J.M., Schutte, W., 1991, A&A, 243, 473-77.
Harris, T.D., Lee, D.H., Blumberg, M.Q., Arumainayagam, C.R., 1995, J. Phys. Chem., 99, 9530-5.
Herbst, E., 1995, Annu. Rev. Phys. Chem. , 46, 27-54.
Herbst, E., 2014, Phys. Chem. Chem. Phys., 16, 3344-59.
Hollis, J.M., Lovas, F.J., Jewell, P.R., 2000, Astrophys. J., 540, L107-L10.
Horn, A., Mollendal, H., Sekiguchi, O., Uggerud, E., Roberts, H., Herbst, E., Viggiano, A.A., Fridgen, T.D., 2004, Astrophys. J., 611, 605-14.
Hudson, R.L., Moore, M.H., 2000, Icarus, 145, 661-63.
Irvine, W.M., Goldsmith, P.F., Hjalmarson, A.A., , 1987, Interstellar processes, Chemical abundances in molecular clouds. Dordrecht D., Reidel Publishing Co, WY.
Jheeta, S., Domaracka, A., Ptasinska, S., Sivaraman, B., Mason, N.J., 2013, Chem. Phys. Lett, 556, 359-64.
Kaplan, I.G., Miterev, A.M., 1987, Adv. Chem. Phys., 68, 255-386.
Kurtz, R.L., Usuki, N., Stockbauer, R., Madey, T.E., 1986, J. Electron Spectrosc., 40, 35-58.
Maity, S., Kaiser, R.I., Jones, B.M., 2015, Phys. Chem. Chem. Phys., 17, 3081-114.
Mangum, J.G., Wootten, A., 1993, ApJS, 89, 123-53.
Mannings, V., Boss, A.P., Russell, S.S., 2000, Protostars and planets iv. University of Arizona Press, Tucson.
Maret, S., Ceccarelli, C., Tielens, A.G.G.M., Caux, E., Lefloch, B., Faure, A., Castets, A., Flower, D.R., 2005, A&A, 442, 527-38.
Oberg, K.I., Garrod, R.T., van Dishoeck, E.F., Linnartz, H., 2009, A&A, 504, 819-913.
Oberg, K.I., Boogert, A.C.A., Klaus, M.P., Saskia van den, B., Ewine, F.v.D., Sandrine, B., Geoffrey, A.B., Neal, J.E., II, 2011, Astrophys. J., 740, 109.
Olano, C.A., Wlamsley, C.M., Wilson, T.L., 1988, A&A, 196, 194-200.
Palumbo, M.E., Castorina, A.C., Strazzulla, G., 1999, A&A, 342, 551.
Pimblott, S.M., LaVerne, J.A., 2007, Radiat. Phys. Chem., 76, 1244-47.
Prasad, S.S., Tarafdar, S.P., 1983, Astrophys. J., 267, 603-09.
Spinks, J.W.T., Woods, R.J., 1990, An introduction to radiation chemistry. Wiley, New York.
van Dishoeck, E.F., Jansen, D.J., Phillips,

T.G., 1993, A&A, 279, 541-66.
Vidali, G., 2013, Chem. Rev., 113, 8762-82.
Watanabe, N., Shiraki, T., Kouchi, A., 2003, Astrophys. J., 588, 121-24.